33rd Annual International Conference of the IEEE EMBS
Boston, Massachusetts USA, August 30 - September 3, 2011

Interactions between cardiac fibrosis spatial pattern and ionic remodeling on electrical wave propagation

Philippe Comtois *Member, IEEE-EMBS* and Stanley Nattel,

Abstract— **Cardiac fibrosis is an important form of pathological tissue remodeling. Fibrosis can electrically-uncouple neighboring excitable cardiomyocytes thus acting as an obstacle to electrical propagation. In this study, we investigated the effects of fibrosis spatial pattern on electrical propagation in control, decreased maximum sodium conductance, and increased intracellular resistivity conditions. Simulations were performed with a monodomain approach and a realistic canine ionic model. We found that the propagation failure is highly dependent on the spatial pattern of fibrosis for all conditions studied with maximum sensitivity for patterns with combination of small and large clusters. However, the effect is particularly sensitive to reduced sodium current condition where conduction block occurred at lower fibrosis density.**

I. Introduction

Atrial fibrillation (AF) is the most common sustained clinical arrhythmia, touching several million Americans. There is evidence pointing to a role for tissue fibrosis in AF maintenance. Atrial fibrosis is associated with conduction abnormalities in experimental congestive heart failure (CHF) in dogs [1, 2]. Spatial dispersion of fibrosis has been shown to be different between systolic and diastolic heart failure in human [3]. Fibrosis occurs most commonly as a reparative process to replace dead cardiomyocytes [4].

The replacement of electrically active atrial myocytes that have died by electrically inactive collagen could result in electrical isolation of surrounding myocytes and the formation of barriers to wave propagation. Variation in fibrosis patterns induced different propagation delays in experiments [5]. Diffuse fibrosis resulted in a decrease in velocity of propagation in both at the 2D and 3D [6, 7]. It has been shown that obstacles can anchor and thus stabilize re-entering electrical activity [8, 9]. The wavefront-boundary interaction is also a key determinant of curvature of the re-entering front, which can influence propagation velocities [10, 11] and refractory periods [11, 12]. A recent study proposed that the spatial pattern of fibrosis may be an important player in AF stabilization [13]; however the understanding of this phenomenon remains limited. In order to better understand the role of the fibrosis spatial pattern and interaction with tissue electrical remodeling, we studied the effect of fibrosis on the propagation of the electrical activity as a function of the density (D_f) and spatial pattern of fibrosis in different conditions (control, decreased sodium current, and increased tissue resistivity).

Manuscript received March 26, 2011. This work was supported in part by the Natural Sciences and Engineering Research Council (P.C.), the Mathematics of Information Technology and Complex Systems (P.C. and S.N.) and the Canadian Institute of Health Research (S.N.).

P. Comtois is a Young investigator Awardee of the "Fonds de la Santé du Québec" with the Department of Physiology/Institute of Biomedical Engineering, Universite de Montreal and Research Centre, Montreal Heart Institute, 5000 Belanger St, Montreal (Quebec), Canada H1T 1C8 (e-mail: philippe.comtois@umontreal.ca).

S. Nattel is with the Department of Medicine, Universite de Montreal and the Research Centre, Montreal Heart Institute.

II. Methodology

A. Stochastic model of fibrosis patterns

We developed a novel simple model with which various patterns of fibrosis clusters can be built. The following sequential steps are repeated to build different 2-D fibrosis patterns with fibrosis density D_f:

1. A random number p is generated from an uniform distribution,
2. A new fibrotic site (100×100 μm^2) will touch an existing fibrotic area if $p > p_{thr}$ *given that open sites satisfying this condition still exists*,
3. The position of the new fibrotic site is randomly chosen in the set of sites respecting the previous condition,
4. *Redo steps 1-3* to increase the density of fibrosis D_f to the desired amount.

The probability for a new site to fall in a site without neighboring fibrosis is thus given by the parameter p_{thr} unless D_f is high enough that all remaining new fibrotic sites will be touching existing clusters.

B. Monodomain representation of atrial tissue

Fibrosis patterns are integrated by replacing cardiac cells (100×100 μm^2) of the discretized 2-D isotropic substrate by holes with no-flux boundary conditions (disconnected space with no leak). A continuous and homogeneous monodomain representation of cardiac tissue was simulated with temporal and spatial variation of the transmembrane potential (V) given by eq.(1):

$$\frac{a}{2r_i}\nabla^2 V = C_m \frac{\partial V}{\partial t} + I_{ion}\left(V,\vec{f}\right) \quad (1)$$

where a =5 μm, r_i = 75 Ohm-cm in control, and C_m=100 μF. I_{ion} was calculated with the ionically-realistic Ramirez-Nattel-Courtemanche canine atrial ionic model[14].We studied three groups of tissue: control (ctl), decreased maximum sodium conductance by 50% ($0.5xG_{Na}$), and increased tissue resistivity to 500 Ohm-cm ($6.66xr_i$). The resulting velocities of propagation from rest are: 92 cm/s (ctl), 65 cm/s ($0.5\times G_{Na}$), and 34 cm/s ($6.66\times r_i$).

C. Measures

The time of activation (T_{act}) of each node of the model is detected by taking the time at which the cell first depolarized over -60 mV. Then, T_{act} is normalized by the time for an electrical wave to propagate from the stimulated side to the opposite of the tissue without fibrosis. Thus, the normalized time of activation (τ_{act}) is defined relative to propagation in a homogeneous tissue with identical resistivity and ionic properties. For direct comparison to the case without fibrosis, the delay of propagation ($delay_{prog}$) is defined as the normalized time τ_{act} when the first cell on the side opposite to the stimulation is activated. Simulations where $delay_{prog}$ exists are flagged as "no block" while a case of "propagation block" corresponds to a simulation where no cell on the side opposite to the stimulation is activated.

The ratio of propagation block (R_{block}) is defined as the number of simulations with propagation block over the total number of simulations for each pair (p_{thr}, D_f). Thus, for each (p_{thr}, D_f), a total of 40 simulations were done (10 different fibrosis patterns × 4 stimulation locations corresponding to each side of the substrate).

For all neighbouring substrate points separated by a distance of 500 μm, the local phase differences in τ_{act} are calculated for phase analysis as described in reference [15]. In summary, of each quadruplet of sites, the largest phase difference normalized by distance is taken, and these values pooled together to populate the maximum phase distribution. Percentile scores at 5%, 50%, and 95%, respectively P_5, P_{50}, and P_{95}, are used to describe the distribution. The heterogeneity index was then calculated as $\text{Index} = (P_{95} - P_5) / P_{50}$.

III. Results

Examples of normalized activation time for a single beat from rest following stimulation of the right side of the substrate with $D_f = 0.2$ is shown in Fig. 1. The $delay_{prog}$, for the first cell to activate on the opposite side are 1.14 for $p_{thr}=0.01$ (panel A) and 1.59 for $p_{thr}=0.125$ (panel B) showing a sensitivity of the delay to the pattern granularity. The increased delay in panel B comes with an increase complexity of isochrones compared to panel A. In general, increasing D_f induces a conduction delay for all p_{thr} as expected.

The ratio of propagation failure (R_{block}) was calculated for p_{thr} between 0.01 and 0.99 and is depicted in Fig. 2A for control substrates. An interesting result is the non-monotonous variation in the minimum D_f for propagation failure to occur ($R_{block} > 0$). First, the minimum D_f for propagation block decreases when increasing p_{thr} from 0.01 to 0.125. The minimum D_f then increases until $p_{thr} = 0.28$ where the minimum density remains constant at 0.37 for p_{thr} between 0.28 and 0.99 (delimited by a white transparent patch). A comparison of the D_f values for $R_{block} = 0.5$ ($D_{f,Rblock=0.5}$) shows that the spatial characteristics of fibrosis can change the minimum D_f by up to ~10% (comparing p_{thr} =0.01 and p_{thr} =0.125).

The region of fig. 2 covered by the semi-transparent white patch shows a almost identical relation between R_{block} and D_f for $p_{thr} > 0.28$. The reason for this invariant behavior seems to be linked to the stochastic model of fibrosis. Thus for a given p_{thr} when increasing D_f starting from 0, the numbers of available sites where a new fibrosis cluster can be created without touching an existing fibrotic cluster decreases to zero differently as a function of p_{thr}. Theoretically, for $p_{thr}=1$ (all clusters need not to touch another cluster), building optimal packing results in a maximum D_f of 0.25 (since packing is still random, the limit D_f is around 0.15). Thus, for large p_{thr}, the limit at which there are no available sites to satisfy the not-touching condition appears at low D_f. Inversely, building patterns with small p_{thr} favors adding patches touching existing clusters leading to higher D_f to attain the limit. Interpretation of the results suggests that the behavior of R_{block} is constant when we reached that limit.

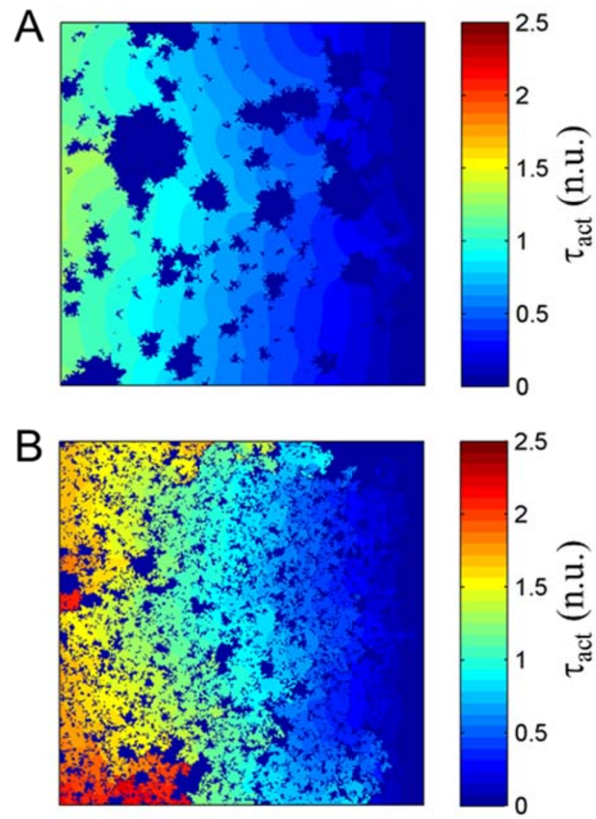

Fig. 1 Examples of propagation obtained from pacing the right side of the substrate with $D_f = 0.2$ for A) $p_{thr} = 0.01$ and B) $p_{thr} = 0.125$.

Results of R_{block} obtained with decreased maximum sodium current ($0.5\times G_{Na}$) are presented in Fig. 2B. A similar non-monotonous variation as in control condition (panel A) is found. $D_{f,Rblock=0.5}$ decreases from 0.32 ($p_{thr} = 0.01$) to 0.18 ($p_{thr} = 0.1$) after increasing to ~0.31. Comparing ctl and $0.5\times G_{Na}$ shows that decreasing G_{Na} results in a decrease of the minimum $D_{f,Rblock=0.5}$ from ~0.32 (ctl) to ~0.18 ($0.5\times G_{Na}$).

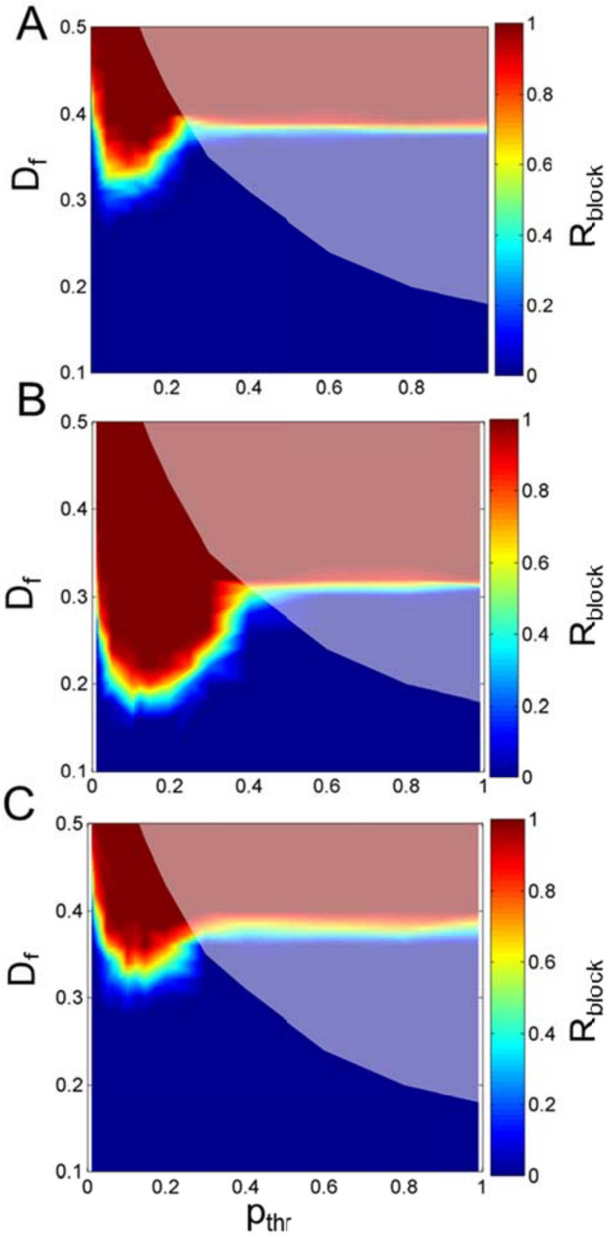

Fig. 2 Ratio of conduction block (R_{block}) as a function of p_{thr} and D_f for A) ctl , B) "0.5×G_{Na}", and C) "6.66×r_i" groups. The area covered by the white semi-transparent patch corresponds to the situation when a new fibrotic patch cannot be added without touching an existing cluster.

Increasing tissue resistivity resulted in a behavior for R_{block} (Fig. 2C) similar to the two previous conditions with again the non-monotonic variation of D_f for conduction block to occur as a function of p_{thr}. A comparison of $D_{f,Rblock=0.5}$ between control and increased resistivity conditions yielded almost identical minimum values of 0.32 but at a lower p_{thr} for tissue with higher resistivity (0.05 for ctl vs. 0.1 for 6.66×r_i). However increasing r_i resulted in higher difference between minimum and maximum $D_{f,Rblock=0.5}$ over all p_{thr} values (~0.10 in ctl vs. ~0.15 for 6.66×r_i). In order to assess the sensitivity to a change in D_f, we calculated for every p_{thr} the interval in D_f between R_{block} = 0.95 and R_{block} = 0.05 ($\Delta D_{f,Rblock}$) as an index. The results obtained show that $\Delta D_{f,Rblock}$ is smaller for the "6.66×r_i" group (maximum $\Delta D_{f,Rblock}$ of 0.13) compared to ctl (maximum $\Delta D_{f,Rblock}$ of 0.16) most predominantly for p_{thr} < 0.1. Thus, increasing tissue resistivity results in a more rapid change in R_{block} when increasing D_f compared to control substrates.

The question remains whether the transition to block of propagation with increasing D_f is solely determined by the heterogeneity of propagation. The heterogeneity index was thus calculated for each p_{thr} at the limit of conduction i.e. at D_f preceding the conduction block. The results are plotted in Fig. 3 for the three groups presented in Fig. 2. The Index for the ctl and the "6.66×r_i" groups increases with p_{thr} similarly. The results were initially fit by $A - Be^{-p_{thr}/\kappa}$ (black curves). Comparison of the fitted parameters show that Index increases less rapidly with increased tissue resistivity (κ = 0.06 in ctl compared to 0.08 for "6.66xr_i"group). Interestingly for the 0.5×G_{Na} group, the Index could not be fitted by a single exponential but required a double exponential of the form $A - Be^{-p_{thr}/\kappa_1} + Ce^{-p_{thr}/\kappa_2}$. The rapid increase in the Index (fig. 3) for is due to κ_1 = 0.04 lower than κ = 0.06 in control followed by a decrease in the index via the second exponential with κ_2 = 0.29.

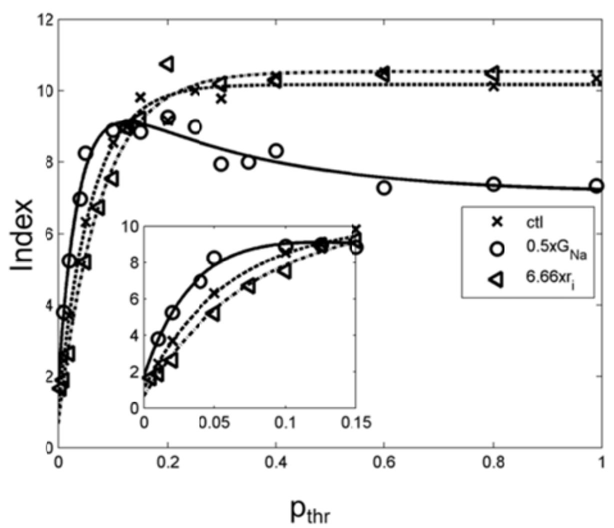

Fig. 3 Mean index of heterogeneity calculated from simulations right before conduction block occurs when increasing D_f. Results obtained for ctl, 0.5×G_{Na} and 6.66×r_i groups are shown. The insert is a close-up view of the index in the range of p_{thr} = 0 to 0.15.

IV. Discussion and Conclusions

Atrial fibrillation occurs more often with aging and cardiac pathologies, correlating with increasing fibrosis. The increase in fibrosis influences both the mechanical and the electrical function of the heart. Clinical studies have suggested a role for fibrotic tissue in partial wave block [16] conduction delays, propagation blocks, and greater conduction heterogeneity [5, 17]. It is believed that the pattern of fibrosis plays a particularly important role [5].

However, how precisely fibrosis pattern alters electrical propagation with and without electrical remodelling remains unclear.

Here we show that independently of the substrate electrical characteristics, the spatial pattern of fibrosis modifies the amount of fibrosis needed for conduction block. However, block of the sodium current results in a shift of R_{block} to lower D_f. Thus, rapid electrical activity or decreased expression of sodium channels will favour conduction block at lower fibrosis density, as is otherwise the case for diffuse fibrosis[18]. Surprisingly, increasing tissue resistivity (resulting in almost 1/3 of the control velocity of propagation) did not have a strong effect on the sensitivity to conduction block and heterogeneity of propagation (see Figs. 2 and 3). An exception is for small p_{thr} where increasing the resistivity seems to favour propagation in tissue with higher fibrosis density accompanied by a decrease in conduction heterogeneity (see insert in fig. 3).

An interesting result is the non-monotone variation in the heterogeneity index that is seen with decreased maximum sodium conductance ($0.5\times G_{Na}$) which peaked in the region where propagation failure occurred at lower D_f (fig. 2). This result is consistent with the usual interpretation that larger conduction heterogeneity is a marker of greater sensitivity to arrhythmia. However, the same interpretation seems not to apply to control and increased tissue resistivity conditions. The exact mechanisms remain to be elucidated.

REFERENCES

[1] D. Li, *et al.*, "Promotion of atrial fibrillation by heart failure in dogs: atrial remodeling of a different sort," *Circulation,* vol. 100, pp. 87-95, 1999.

[2] T. J. Cha, *et al.*, "Dissociation between ionic remodeling and ability to sustain atrial fibrillation during recovery from experimental congestive heart failure," *Circulation,* vol. 109, pp. 412-8, Jan 27 2004.

[3] B. Lopez, *et al.*, "Alterations in the pattern of collagen deposition may contribute to the deterioration of systolic function in hypertensive patients with heart failure," *J Am Coll Cardiol,* vol. 48, pp. 89-96, Jul 4 2006.

[4] M. A. Silver, *et al.*, "Reactive and reparative fibrillar collagen remodelling in the hypertrophied rat left ventricle: two experimental models of myocardial fibrosis," *Cardiovasc Res,* vol. 24, pp. 741-7, Sep 1990.

[5] T. Kawara, *et al.*, "Activation delay after premature stimulation in chronically diseased human myocardium relates to the architecture of interstitial fibrosis," *Circulation,* vol. 104, pp. 3069-75, Dec 18 2001.

[6] K. H. ten Tusscher and A. V. Panfilov, "Influence of nonexcitable cells on spiral breakup in two-dimensional and three-dimensional excitable media," *Phys Rev E Stat Nonlin Soft Matter Phys,* vol. 68, p. 062902, 2003.

[7] K. H. W. J. t. Tusscher and A. V. Panfilov, "Wave Propagation in Excitable Media with Randomly Distributed Obstacles," *Multiscale Modeling & Simulation,* vol. 3, pp. 265-282, 2005.

[8] J. M. Pastore and D. S. Rosenbaum, "Role of structural barriers in the mechanism of alternans-induced reentry," *Circ Res,* vol. 87, pp. 1157-63, 2000.

[9] P. Comtois and A. Vinet, "Multistability of reentrant rhythms in an ionic model of a two-dimensional annulus of cardiac tissue," *Phys Rev E Stat Nonlin Soft Matter Phys,* vol. 72, p. 051927, 2005.

[10] V. S. W. A. T. Zykov, *Simulation of wave processes in excitable media*: Manchester : Manchester University Press, 1987.

[11] P. Comtois and A. Vinet, "Curvature effects on activation speed and repolarization in an ionic model of cardiac myocytes," *Phys Rev E,* vol. 60, pp. 4619-28, 1999.

[12] K. J. Sampson and C. S. Henriquez, "Interplay of ionic and structural heterogeneity on functional action potential duration gradients: Implications for arrhythmogenesis," *Chaos,* vol. 12, pp. 819-828, 2002.

[13] K. Tanaka, *et al.*, "The Spatial Distribution of Fibrosis Governs Fibrillation Wave Dynamics in the Posterior Left Atrium During Heart Failure," *Circ Res,* Aug 17 2007.

[14] R. J. Ramirez, *et al.*, "Mathematical analysis of canine atrial action potentials: rate, regional factors, and electrical remodeling," *Am J Physiol,* vol. 279, pp. H1767-85, 2000.

[15] W. J. Lammers, *et al.*, "Quantification of spatial inhomogeneity in conduction and initiation of reentrant atrial arrhythmias," *Am J Physiol,* vol. 259, pp. H1254-63, Oct 1990.

[16] T. J. Wu, *et al.*, "Relation between cellular repolarization characteristics and critical mass for human ventricular fibrillation," *J Cardiovasc Electrophysiol,* vol. 10, pp. 1077-86, 1999.

[17] B. Burstein, *et al.*, "Changes in connexin expression and the atrial fibrillation substrate in congestive heart failure," *Circ Res,* vol. 105, pp. 1213-22, Dec 4 2009.

[18] K. H. Ten Tusscher and A. V. Panfilov, "Influence of diffuse fibrosis on wave propagation in human ventricular tissue," *Europace,* vol. 9 Suppl 6, pp. vi38-45, Nov 2007.